Mass transfer studies at packed bed rotating cylinder electrodes of woven-wire meshes

J. M. GRAU and J. M. BISANG*

Programa de Electroquímica Aplicada e Ingeniería Electroquímica (PRELINE), Facultad de Ingeniería Química (UNL), Santiago del Estero 2829, S3000AOM, Santa Fe, Argentina
(*author for correspondence E-mail: jbisang@fiqus.unl.edu.ar)

Abstract

Mass transfer has been studied at rotating cylinder electrodes of woven-wire meshes using the reduction of ferricyanide as test reaction. The experimental data are well correlated by an empirical expression between the Sherwood number and the Reynolds number, both in terms of the hydraulic diameter as characteristic length, and including two additional dimensionless parameters in order to characterize the geometry of the meshes. The mass-transfer enhancement factor for three-dimensional electrodes is analyzed.

List of Symbols

a constant in Equation 2
A_s specific surface area (m^{-1})
C concentration (mol m^{-3})
d external cylinder diameter (m)
d_h hydraulic diameter $= 4\varepsilon/A_s$
D diffusion coefficient ($m^2\ s^{-1}$)
F Faraday constant (C mol^{-1})
H distance between wires (m)
I_{lim} limiting current (A)
k_m mass-transfer coefficient (m s^{-1})
r_1 internal radius (m)
r_2 external radius (m)
$\bar{r}$ mean radius $= \sqrt{(r_1^2 + r_2^2)/2}$ (m)
Re_d Reynolds number in terms of d as characteristic length $= \omega r_2 d/v$

Re Reynolds number $= \omega r_2 d_h/v$
Sc Schmidt number $= v/D$
Sh_d Sherwood number in terms of d as characteristic length $= k_m d/D$
Sh Sherwood number $= k_m d_h/D$
V_e electrode volume (m^3)

Greek Symbols

α exponent of the Reynolds number in Equation 2
ε porosity
κ exponent of a dimensionless parameter in Equation 2
v kinematic viscosity ($m^2\ s^{-1}$)
v_e charge number of the electrode reaction
ω rotation speed (rpm or s^{-1})

1. Introduction

Electrochemical reactors with rotating cylinder electrodes are proposed for the treatment of effluents [1] due to their good mass-transfer conditions produced by the movement of the electrode. However, in order to further increase the space time yield the incorporation of turbulence promoters has been suggested. Thus, Kappesser et al. [2] performed mass-transfer investigations at rotating cylinders with staggered diamond knurls machined on their surfaces. Sedahmed et al. [3] studied mass-transfer at rotating finned cylinders, where fins were made by cutting longitudinal rectangular grooves in the cylinder. Makanjuola and Gabe [4] reported mass-transfer studies at V-grooved cylinders and the investigation was extended to pyramidal knurling and wires or meshes wound to the cylindrical rotating electrode [5]. Further mass-transfer works as a function of the roughness factor are discussed by Gabe et al. [6]. Like other rotating electrode geometries, the three-dimensional rotating cylinder electrode pumps the electrolyte from the bottom of the cell to the top. Thus, another strategy for employing rotating cylinder electrodes is to make use of the electrolyte flow through the electrode.

Nahlé et al. [7] reported mass-transfer data for rotating cylinder electrodes of reticulated vitreous carbon. Using copper deposition as test reaction they found that the limiting current was dependent upon velocity to the power 0.55 to 0.71 depending upon the porosity of the carbon foam. Grau and Bisang [8] studied the performance of electrochemical reactors with rotating cylinder electrodes of expanded metal. Using the ferricyanide reduction as test reaction they reported that the Sherwood number was dependent on the Reynolds number, both defined in terms of the hydraulic diameter as characteristic length, to the power 0.63. To take into account the geometry of the expanded metal two additional dimensionless parameters were included in the empirical expression. Kreysa [9, 10] investigated the behaviour of a rotating packed bed cell with an external radial flow of electrolyte superimposed on the electrolyte flow induced by the electrode movement. A dependence of the Sherwood number on both Reynolds numbers, convective and rotational, to the power 0.58 was reported. A comparison of the mass-transfer characteristics of three dimensional rotating electrodes against smooth and rough electrodes was performed and it was concluded that the mass-transfer coefficients are about three times higher than those obtained with smooth rotating cylinder electrodes at the same conditions [8, 11].

Several investigations of the behaviour of mesh electrodes have been published [12]. Mesh electrodes present a higher specific surface area and promote turbulence in the electrolyte flowing over them [13]. The aim of the present work is to quantify the mass-transfer to a rotating cylinder electrode of woven-wire meshes and to compare the mass-transfer characteristics with similar rotating structures.

2. Experimental details

The experiments were performed in an undivided batch reactor (95 mm int. dia. and 140 mm high) maintained at constant temperature by a heating jacket. Figure 1 shows the configuration of the electrochemical reactor used. The working electrode was a rotating cylinder (35 mm int. dia.) made by ordered packing of woven-wire meshes of 316 stainless steel plated with nickel [8]. Nine types of mesh were used; their geometrical characteristics, measured in the laboratory, are summarized in Table 1 named by mesh size. The mesh size 14 represents a special case with a thinner wire diameter, which was included in order to corroborate the mass-transfer study. The lower part of the electrode was open but the upper part was joined to a Teflon sleeve in order to orientate the electrolyte flow through the sheet pack. A perforated Teflon disc, centrally positioned, was used as support of the three-dimensional electrode. A nickel plated stainless steel bolt passed through the bed thickness, pressing the electrode shaft and thus ensuring electric contact. A concentric helical nickel wire (1.5 mm
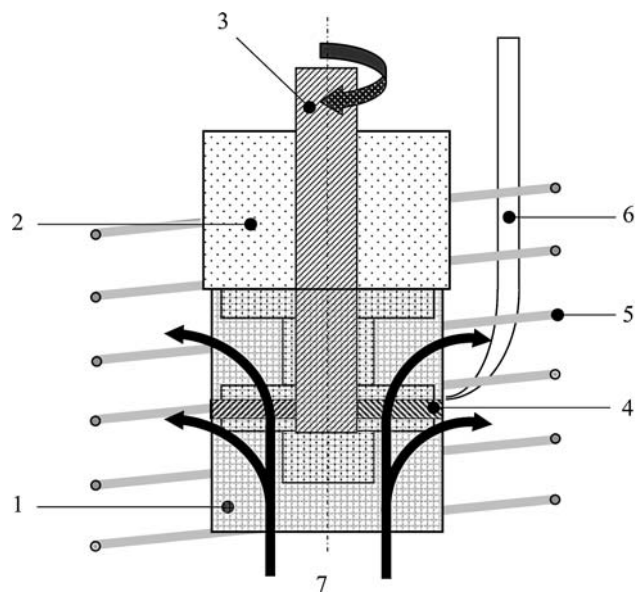

Fig. 1. Schematic view of the electrochemical reactor. (1) working electrode, (2) Teflon sleeve, (3) electrode shaft, (4) electric contact, (5) anode, (6) Luggin capillary and (7) electrolyte flow rate produced by the electrode rotation.

dia. × 190 cm long) with an interelectrode gap of 20 mm was used as counterelectrode, while the reference electrode was a saturated calomel electrode. The potential was controlled against the reference electrode connected to a Luggin capillary positioned at the middle of the outer face of the three-dimensional cathode.

The test reaction was the electrochemical reduction of ferricyanide from solutions with $[K_3Fe(CN)_6] \cong 5 \times 10^{-4}$ M, $[K_4Fe(CN)_6] \cong 5 \times 10^{-2}$ M, in 1 M NaOH or 3 M NaOH as supporting electrolyte, while the reverse reaction occurs at the anode. The cathode potential was swept from the open circuit potential (typically 100 mV vs SCE for 1 M NaOH and 125 mV for 3 M NaOH) to a value of −400 mV vs SCE and the current against potential curve was then recorded at a sweep rate of 1 mV s^{-1}. In all cases a well defined limiting current was observed. Samples of the solution were taken from the reactor after each experiment and the ferricyanide concentration was spectrophotometrically determined using a Perkin-Elmer model Lambda 20 double-beam UV–Vis Spectrophotometer with 10 mm glass absorption cells and as blank the supporting electrolyte was used. The measurements were performed at a wavelength of 430 nm, where it is possible to determine the ferricyanide concentration without interference of ferrocyanide. In a set of experiments the above procedure was repeated for five values of rotation speed in a given electrolyte. After two sets of experiments the nickel coating was stripped by acid immersion [14] and the electrode was plated with a fresh nickel surface. The experiments were performed at 30 °C and nitrogen was bubbled in the reactor for 1 h prior to the experiment in order to remove the dissolved oxygen.

Table 1. Geometrical parameters of the electrodes

Mesh size	5	8	10	14	18	30	40	60	100
Wire diameter/mm	1	0.7	0.6	0.3	0.4	0.25	0.22	0.17	0.1
Distance between wires, H/mm	4.080	2.475	1.940	1.514	1.011	0.597	0.415	0.253	0.154
Number of sheets	1	2	2	2	2	2	2	2	2
Apparent thickness/mm	2	2.4	2.3	1.2	1.6	1	0.85	0.55	0.35
Specific surface area, A_s/m^{-1}	649	1014	1107	1682	2012	3961	5582	9214	13482
Porosity, ε	0.838	0.823	0.834	0.874	0.799	0.752	0.693	0.597	0.663
Electrode length/mm	40	42	42	41.8	42	40.5	41	40.8	40.3
Number of sheets	2	4	4	4	4	6	4	4	4
Apparent thickness/mm	4	4.75	3.9	2	3.2	3	1.63	1.10	0.7
Specific surface area, A_s/m^{-1}	649	1024	1306	2018	2012	3961	5821	9214	13482
Porosity, ε	0.838	0.821	0.804	0.849	0.799	0.752	0.68	0.597	0.663
Electrode length/mm	40	42	43	42	42	40.5	41	40.6	41

In all the experiments the bed thickness of the three-dimensional electrode was lower than the value given by Kreysa [15]. Thus, the whole bed is working under limiting current conditions and the mass-transfer coefficient was calculated from the limiting current and reactant concentration using the following equation [16]

$$k_m = \frac{I_{\lim}}{v_e F V_e A_s C} \qquad (1)$$

Further details of the electrode coating and electrolyte properties can be obtained from previous work [8].

3. Mass-transfer analysis

For rotating three-dimensional electrodes the mass-transfer conditions can be described by a dimensionless group correlation of the form [8]

$$\mathrm{Sh} = a\left(\mathrm{Re} \times \frac{r_2}{\bar{r}}\right)^{\alpha} \mathrm{Sc}^{1/3} \left(\frac{H}{\bar{r}}\right)^{\kappa} \qquad (2)$$

where Sh and Re are the Sherwood and Reynolds numbers respectively in terms of the hydraulic diameter as characteristic length, Sc is the Schmidt number, $r_2/\bar{r}$ and $H/\bar{r}$ are additional geometric relations in order to take into account the characteristics of the three-dimensional electrode of woven-wire mesh. The distance between wires, H, is a measure of the distance between consecutive turbulence promoters and the external radius, r_2, takes into account the effect of the electrode size. Both H and r_2 are related to $\bar{r}$, which depends on the internal radius and on the electrode thickness.

4. Results and comparisons

Figure 2 shows double logarithmic plots of Equation 2. Table 2 reports the correlation parameters according to the least squares method applied to each set of experimental points. α is close to 0.6 in all cases in accordance with previous studies [7, 8, 10] performed with rotating three-dimensional electrodes.

The constant a and the exponents α and κ in Equation 2 were determined using a linear multiparametric

correlation adjusting the experimental points to the logarithmic form of Equation 2. Thus, the 163 experimental data of the present study fit the equation:

$$\mathrm{Sh} = 0.967\left(\mathrm{Re} \times \frac{r_2}{\bar{r}}\right)^{0.58} \mathrm{Sc}^{1/3} \left(\frac{H}{\bar{r}}\right)^{0.47} \qquad (3)$$

with a correlation coefficient of 0.97 and 0.081 as standard deviation. Figure 3 compares the experimental results with the correlation values according to Equation 3. Attempts to obtain an empirical expression in terms of other relationships between the geometrical parameters did not produce a better correlation.

To provide comparison with existing mass-transfer data at rotating cylinder electrodes it is convenient to re-write Equation 3 with the Sherwood and Reynolds numbers in terms of the external cylinder diameter as characteristic length. Thus Equation 3 is transformed to

$$\mathrm{Sh}_d = 0.967\mathrm{Re}_d^{0.58}\, \mathrm{Sc}^{1/3} \times \left(\frac{d_h}{2\bar{r}}\right)^{0.58}\left(\frac{d}{d_h}\right)\left(\frac{H}{\bar{r}}\right)^{0.47} \qquad (4)$$

Equation 4 has the same form as that of the Eisenberg et al. [17] equation, valid for smooth rotating cylinder electrodes, multiplied by a geometric factor; which takes into account the characteristics of the three-dimensional electrode.

In order to determine the efficiency of the woven-wire meshes a mass-transfer enhancement factor can be defined as the ratio between the mass-transfer coefficient for the three-dimensional electrode, Equation 4, and the mass-transfer coefficient at a smooth rotating cylinder electrode [17]. Figure 4 shows the enhancement factor as a function of the Reynolds number, in terms of the cylinder diameter as characteristic length, and the Schmidt number. The enhancement factor ranges from 2.5 to 3.7 depending mainly on the Reynolds number; the greater the Reynolds number the smaller is the enhancement factor for a given Schmidt number.

Figure 5 shows the enhancement factor as a function of the Reynolds number for different three-dimensional structures. The enhancement factor according to the Holland expression [18], valid for metal powder deposition, is included in Figure 5. In Figure 5 for the mass-transfer expressions proposed by Kreysa [10],
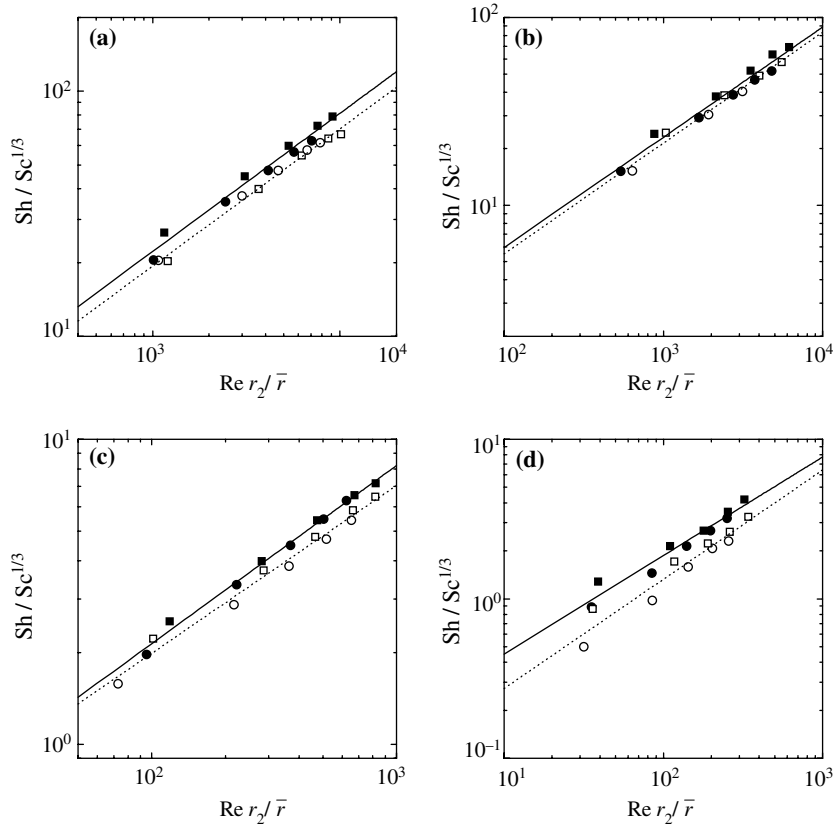
Fig. 2. Typical Sherwood–Reynolds correlations. (a) Mesh size 5, (b) mesh size 8, (c) mesh size 40 and (d) mesh size 100. For (a): (■): 1 sheet, 1 M NaOH. (●):1 sheet, 3 M NaOH. (□) : 2 sheets, 1 M NaOH, (○):2 sheets, 3 M NaOH. Full line: correlation for 1 sheet. Dotted line: correlation for 2 sheets. For (b), (c) and (d): (■): 2 sheets, 1 M NaOH. (●):2 sheets, 3 M NaOH. (□): 4 sheets, 1 M NaOH, (○):4 sheets, 3 M NaOH. Full lines: correlation for 2 sheets. Dotted lines: correlation for 4 sheets.

Grau and Bisang [8] and for Equation 4 of this study a geometric factor is necessary, which allows the correlations to be rewritten in terms of the Sherwood and Reynolds numbers according to Eisenberg et al. [17]. A value of 1.05 was adopted for the geometric factor in the Kreysa equation, 0.42 for the relationship reported in [8] and 1 for the correlation of this study, which represent mean values for the geometrical arrays. It can be observed that the enhancement factor for three-dimensional electrodes is close to three, and it is very similar for the different materials used for the electrodes. Likewise, the enhancement factor decreases as the Reynolds number increases, because the exponent of the Reynolds number for three-dimensional electrodes is lower than for smooth electrodes. Likewise, it can be seen that the enhancement factors for three-dimensional electrodes are lower than the values for metal powder deposition.

Table 2. Summary of correlation parameters

Mesh size	Sheet number	$a \times (H/\bar{r})^K$	α	Correlation coefficient	Standard deviation
5	1	0.451	0.56	0.990	0.065
	2	0.402	0.56	0.997	0.037
8	2	0.399	0.59	0.984	0.088
	4	0.362	0.59	0.990	0.070
10	2	0.666	0.51	0.994	0.050
	4	0.299	0.58	0.990	0.068
14	2	0.521	0.49	0.994	0.047
	4	0.381	0.55	0.983	0.085
18	2	0.255	0.62	0.994	0.058
	4	0.255	0.57	0.997	0.039
30	2	0.146	0.60	0.999	0.024
	6	0.182	0.60	0.999	0.012
40	2	0.145	0.58	0.997	0.036
	4	0.158	0.55	0.992	0.059
60	2	0.086	0.65	0.999	0.019
	4	0.089	0.60	0.977	0.110
100	2	0.109	0.62	0.976	0.113
	4	0.057	0.68	0.967	0.156

5. Conclusions

The experimental results of mass-transfer at rotating cylinder electrodes of woven wire meshes are well correlated by a dimensionless equation involving the Sherwood and Reynolds number, in terms of the hydraulic diameter as characteristic length, the Schmidt number and two additional parameters, $r_2/\bar{r}$ and $H/\bar{r}$, characterizing the geometry of the three-dimensional structure.
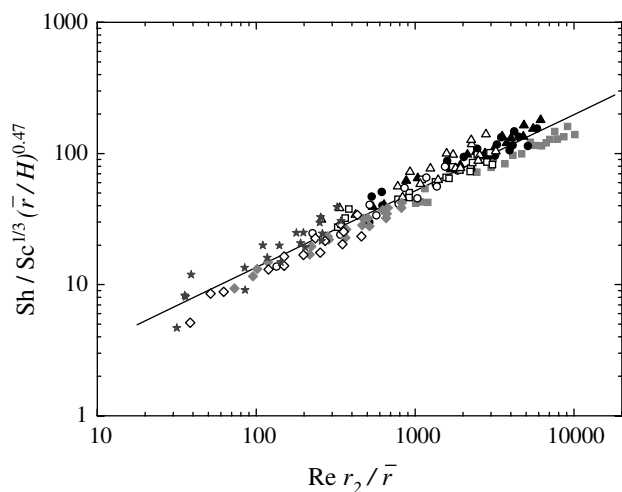
Fig. 3. Mass-transfer data against Reynolds number for the nine types of mesh size. (■) Mesh size 5, (▲) mesh size 8, (●) mesh size 10, (□) mesh size 14, (△) mesh size 18, (○) mesh size 30, (◆) mesh size 40, (◇) mesh size 60 and (★) mesh size 100. Full line: Equation 3.
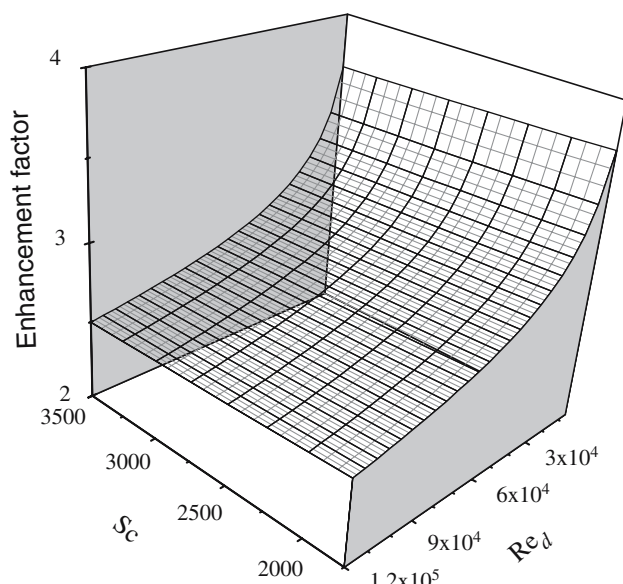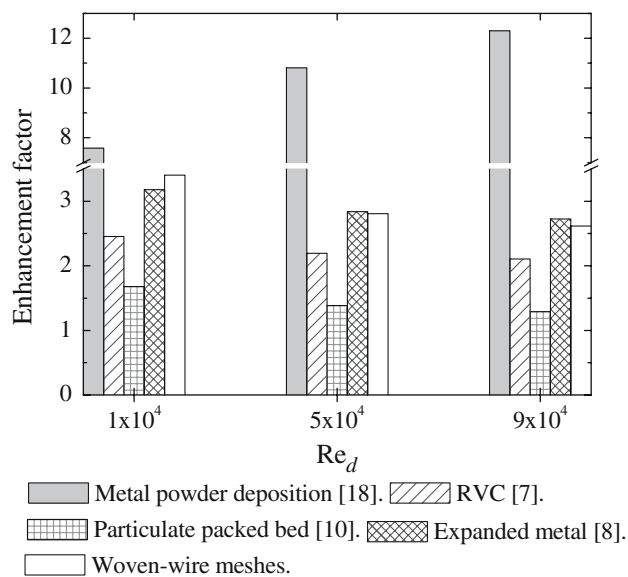

Fig. 5. Comparison of mass-transfer correlations for rotating cylinder electrodes. Reynolds number is given in terms of the diameter of the rotating electrode as characteristic length. Sc = 2000.

Fig. 4. Mass-transfer enhancement factor for the woven-wire mesh electrodes as a function of the Reynolds and Schmidt numbers.

The mass-transfer coefficients for rotating cylinder electrodes of woven-wire meshes are about three times higher than those obtained with smooth electrodes, because of the turbulence promoting action of the meshes.

Acknowledgements

References

1. F.C. Walsh, in D. Genders and N. Weinberg (Eds), 'Electrochemistry for a Cleaner Environment', (The Electrosynthesis Company, New York, 1992), pp 101–159.
2. R. Kappesser, I. Cornet and R. Greif, J. Electrochem. Soc. 118 (1971) 1957.
3. G.H. Sedahmed, A. Abdel Khalik, A.M. Abdallah and M.M. Farahat, J. Appl. Electrochem. 9 (1979) 563.
4. P.A. Makanjuola and D.R. Gabe, Surf. Technol. 24 (1985) 29.
5. P.A. Makanjuola and D.R. Gabe, J. Appl. Electrochem. 17 (1987) 370.
6. D.R. Gabe, G.D. Wilcox, J. Gonzalez-Garcia and F.C. Walsh, J. Appl. Electrochem. 28 (1998) 759.
7. A.H. Nahlé, G.W. Reade and F.C. Walsh, J. Appl. Electrochem. 25 (1995) 450.
8. J.M. Grau and J.M. Bisang, J. Appl. Electrochem. 35 (2005) 285.
9. G. Kreysa and R. Brandner, in 'Modern Concepts in Electrochemical Reactor Design', Extended Abstracts of the 31st ISE Meeting, Venice, Italy, 2 (1980) H8.
10. G. Kreysa, Chem.-Ing.-Tech. 55 (1983) 23(In German).
11. C.T. John Low, C. Ponce de Leon and F.C. Walsh, Aust. J. Chem. 58 (2005) 246.
12. F. Coeuret and A. Storck (1984). Elements de Genie Electrochimique (TEC&DOC, Paris, 1984), chapter 3, p. 159.
13. J. Cano and U. Böhm, Chem. Eng. Sci. 32 (1977) 213.
14. E.B. Saubestre, in F.A. Lowenheim (Ed.), 'Modern Electroplating', (John Wiley & Sons, New York, 1974), 3rd ed., chapter 32, p. 762.
15. G. Kreysa, DECHEMA Monographs 94 (1983) 123(in German).
16. F.C. Walsh, 'A First Course in Electrochemical Engineering' (Alresford Press, Alresford, 1993), chapter 5, p. 149.
17. M. Eisenberg, C.W. Tobias and C.R. Wilke, J. Electrochem. Soc. 101 (1954) 306.
18. F.S. Holland, Chem. Ind. (London) July (1978) 453.